Monthly Notices
of the
ROYAL ASTRONOMICAL SOCIETY

Mon. Not. R. Astron. Soc. **425,** 701–708 (2012) doi:10.1111/j.1365-2966.2012.21559.x

Red is the new black: how the colour of urban skyglow varies with cloud cover

C. C. M. Kyba,[1,2]★ T. Ruhtz,[1] J. Fischer[1] and F. Hölker[2]

[1]*Institute for Space Sciences, Freie Universität Berlin, Carl-Heinrich-Becker-Weg 6-10, D-12165 Berlin, Germany*
[2]*Leibniz-Institute of Freshwater Ecology and Inland Fisheries, D-12587 Berlin, Germany*

Accepted 2012 June 20. Received 2012 April 26; in original form 2012 January 19

ABSTRACT

The development of street lamps based on solid-state lighting technology is likely to introduce a major change in the colour of urban skyglow (one form of light pollution). We demonstrate the need for long-term monitoring of this trend by reviewing the influences it is likely to have on disparate fields. We describe a prototype detector which is able to monitor these changes, and could be produced at a cost low enough to allow extremely widespread use. Using the detector, we observed the differences in skyglow radiance in red, green and blue channels. We find that clouds increase the radiance of red light by a factor of 17.6, which is much larger than that for blue (7.1). We also find that the gradual decrease in sky radiance observed on clear nights in Berlin appears to be most pronounced at longer wavelengths.

Key words: radiative transfer – atmospheric effects – instrumentation: detectors – light pollution.

1 INTRODUCTION

The development of artificial lighting has allowed humans to extend the hours of activity well into the night. In the ideal case, street lighting allows pedestrians to safely navigate at nighttime, by reflecting light by the ground and nearby objects. The vast majority of this reflected light, however, is not detected by a human eye, and much of it instead propagates into the sky. In the worst cases, improperly designed light fixtures radiate much of their light directly into the sky, often causing glare and potentially hindering navigation. Upward-directed light can undergo scattering off of molecules (Rayleigh scattering) or aerosols, causing the unintended phenomena of skyglow, a type of light pollution. Urban skyglow has fundamentally altered the character of the night, as can be seen in Fig. 1.

The extremely deleterious impact of skyglow on the field of visible light astronomy is well documented, and the first quantitative monitoring studies were undertaken in the 1960s and 1970s (Walker 1970; Bertiau, de Graeve & Treanor 1973; Riegel 1973; Berry 1976). The negative externalities of public lighting [e.g. greenhouse gas emissions (Gallaway, Olsen & Mitchell 2010), obsolescence of astronomical research facilities (Riegel 1973), cultural impacts (Gallaway 2010), and potential ecosystem (Rich & Longcore 2006) and human health effects (Navara & Nelson 2007)] are not immediately apparent, and are often difficult to quantify. Furthermore, technological improvements over the last century have repeatedly reduced the direct cost of lighting (per lumen), often leading to increased light levels rather than saved energy (rebound effect) (Herring & Roy 2007; Hölker et al. 2010). As a result, the amount of lighting has increased at a rate of 3–6 per cent per year (Narisada & Schreuder 2004; Hölker et al. 2010), and in 2001 it was estimated that approximately 10 per cent of the world's population, and more than 40 per cent of the US population, no longer viewed the night sky with dark adapted vision (Cinzano, Falchi & Elvidge 2001).

Over the same period that many areas of the globe became permanently lit, chronobiologists learned that regular exposure to darkness is critical to the health of diurnal animals[1] (Navara & Nelson 2007). Briefly, the absence of light is required for the synthesis of melatonin (Reiter et al. 2011), which regulates the circadian rhythm and is a powerful antioxidant. The stress produced by acute disruption of the circadian rhythm will be familiar to any reader who has experienced jet lag. The study of the effects of chronic exposure to unnaturally high levels of light at night is a very active research field (Reddy & O'Neill 2010; Gooley et al. 2011; Meng et al. 2011; Wyse et al. 2011). While most studies on the biological impact of light at night are concerned with the effects of direct light (e.g. Lewy et al. 1980; Salmon et al. 1995), it has been demonstrated that scattered skyglow has ecological impacts (Moore et al. 2000), and the potential for a connection between the level of urban lighting and some human cancers is under investigation (Kloog et al. 2008, 2009; Kantermann & Roenneberg 2009).

1.1 Need for long-term multispectral measurements

The wavelength distribution of street lighting depends upon the chosen lighting technology (Elvidge et al. 2010). In his 1973 letter,

★E-mail: christopher.kyba@wew.fu-berlin.de

[1] Remarkably, the need for darkness extends even to some animals lacking visual systems (Haim et al. 1983).

Figure 1. Comparison of natural and artificially illuminated skies. In pristine areas the night sky is filled with stars on a black background, and clouds appear black. In urban areas stars are washed out by light pollution, and clouds look red or orange. Photo at the left is taken by Ray Stinson in Glacier National Park, and photo at the right is taken by Christopher Kyba in Berlin (Kyba et al. 2011a). Image is released under the Creative Commons Attribution-Share Alike 3.0 Unported license at http://userpage.fu-berlin.de/kyba/images/night_cloud_comparison.html.

Riegel lamented the fact that quantitative light pollution monitoring had not begun prior to the widespread switch from incandescent to vapour lamps (Riegel 1973). Today, the developed world stands once again on the cusp of a potential widespread colour change, this time to white light-emitting diode (LED) street lights (International Dark-Sky Association 2010). There are three major advantages of LED lighting over traditional gas discharge lamps that are likely to lead to their widespread adoption. First, the directional distribution of LED lamps is remarkably customizable, allowing for very precise lighting, with sharp cut-offs to prevent light from being directed where it is unneeded or unwanted. Secondly, in contrast to vapour lights, LED lights can be both dimmed and switched off and on immediately. This trait allows for potential energy savings through reduction of light at times of no human activity. Thirdly, some white LED lights allow good colour rendering, which is generally desired by the public.

This change to LED lighting, which is already underway in many cities (Espen 2011), can be expected to have several consequences. Near the lights themselves, the attraction of insects to LED lights is expected to be different from the current technology, and is currently under investigation (Perkin et al. 2011). In the sky, if all else remained equal then a shift in the public lighting spectrum towards blue will result in more light pollution at zenith and near the sources (International Dark-Sky Association 2010; Kocifaj 2011), due to the stronger Rayleigh scattering at short wavelengths. However, since the angular distribution of LED lights will be very different from the current technology, and presumably more likely to incorporate a full cut-off design, the impact a change of lighting technology would have on skyglow is not obvious. Next, the luminance of skyglow has been shown to be variable in some cities (McKenna 2008; Luginbuhl et al. 2009; Kyba et al. 2011a), but the origin of these gradual changes has not been demonstrated. If municipalities make use of the dimming capabilities of LED lighting, this could potentially introduce a stronger time dependence in sky luminance over the course of individual nights. Finally, blue light is in general much more disruptive to the circadian rhythms of humans (Brainard et al. 2001; Rea et al. 2010), so the disruptive effect of exposure to blue-rich street light and skyglow may be larger than for current technologies (Falchi et al. 2011).

Given the potential rapidity of a change in nightscapes worldwide, it is clear that there is a pressing need for both measurement of the current situation and monitoring of trends. In order for measurements to be taken around the globe, a future multispectral skyglow monitor should be easy to operate, inexpensive, temperature stable, calibratable and robust. The primary aim of this paper is to demonstrate that long-term, multispectral monitoring of the night sky luminance can be accomplished by combining existing inexpensive broad-band light pollution meters with filters. We hope that by demonstrating the need for, and the scientific capabilities of such a detector, manufacturers will be encouraged to bring similar devices to market.

1.2 Overview of current light pollution detectors

1.2.1 Multispectral detectors

The ultimate tool for long-term monitoring of light pollution is an imaging spectrometer installed in a robust housing (e.g. SAND; Aubé 2007). Such a device is capable of not only recording the spectrum of light pollution at high wavelength and temporal resolution, but also the angular distribution of the skyglow. The obvious downside of such an instrument is its extremely high cost, restricting its use to a few select cities.

The next best device for monitoring light pollution is a digital camera using a moving mount or fisheye lens with scientific grade filters (e.g. Duriscoe, Luginbuhl & Moore 2007; Falchi 2010). Compared to an imaging spectrometer, these devices trade reduced spectral resolution for increased spatial resolution. In addition, they have the major advantage that the images can be gain calibrated, and the sky's light extinction profile can be measured offline using star photometry. Once again, cost and complexity of operation preclude such devices from seeing widespread use.

Standard digital cameras (Zotti 2007; Kolláth 2010), including cell phone cameras (Sumriddetchkajorn & Somboonkaew 2010), can also be used to measure light pollution. Because these cameras have filters for red, green and blue light, it is in principle possible to make multispectral measurements using them. Although digital cameras are now ubiquitous, their immediately obvious downside is the wide range of models, lenses and file formats, as well as likely temperature dependencies. While calibration issues make the digital camera of any given member of the public unsuitable for collaborative scientific work, they are excellent devices for individual citizen science initiatives. Mosaics made by taking images with identical camera settings at different locations provide compelling demonstrations of the intensity of light pollution in urban areas.

1.2.2 Broad-band detectors

The human eye has excellent night vision sensitivity, and its ubiquity exceeds even that of digital cameras. The Globe at Night campaign (Walker et al. 2008) provides citizen scientists with star charts displaying the sky under different light pollution levels, along with a simple web interface for reporting observations. In 2011, the campaign recorded 14 249 observations in 115 countries (www.globeatnight.org). While this technique provides the best worldwide coverage possible for surface-based light pollution measurements, its downsides are that measurements are made in a single spectrum range, are not made at identical times, changes in skyglow over the night are not necessarily tracked, factors which reduce the 'seeing' could be confused with actual light, and differences in eyesight or dark adaptation may result in different viewers rating the stellar visibility differently. Nevertheless, if the campaign continues it will produce an intriguing time series with global reach.

There are three broad-band meters that have been developed specifically for the purpose of long-term monitoring of the night sky at multiple sites. Of the three, the most precise is the Night Sky Brightness Monitor (NSBM), which has been developed by the

International Dark Sky Association (McKenna 2008). The NSBM is designed to measure sky luminance at several sites to an accuracy of ±1 per cent over a period of 30 years, as part of a long-term monitoring campaign. It is a luminance meter with two detectors, allowing two different viewing directions. Due to costs stemming from both the manufacture of the precision instrument and the maintenance of accurate calibration over several decades, it is unlikely that the device will be deployed at more than a few dozen carefully chosen locations.

The other two broad-band light meters meet the demands of being easy to operate, inexpensive and robust: The International Year of Astronomy (IYA) lightmeter, manufactured by K2W Lights KG, and the Sky Quality Meter (SQM), manufactured by Unihedron. The IYA lightmeter is effectively a solar panel that has been configured for use as an irradiance meter, and after calibration it reports its measurement in W m^{-2}. Its spectral response is from approximately 320–720 nm, with response at least 50 per cent of the peak from approximately 390–620 nm. Since it measures irradiance in day as well as night, changes in the response (from e.g. dust deposition) can be calibrated using the direct light of the Sun. It is a flat detector, so angular acceptance is the highest at the zenith and decreases towards the horizontal due to both the cosine and specular reflection. The lightmeter is weatherproof, and can be installed without any housing.

The photosensitive element of the SQM is a TAOS TSL237S light to frequency converter, an inexpensive silicon photodiode. The detector is covered by a HOYA CM-500 filter to minimize the influence of infrared (IR) light. The SQM has a response from approximately 320–700 nm, with at least 50 per cent response from approximately 390–630 nm (Cinzano 2005). A temperature sensor in the SQM is mounted near the TSL237S to allow for compensation for the photodetector's known temperature dependence. There are multiple versions of the SQM available; in this work we consider only the SQM-LU, a USB version that uses a lens to reduce the angular acceptance to 10° (half width half maximum) from the zenith.

The SQM is a luminance meter, and reports measurements in the astronomical units of magnitudes per square arcsecond (mag arcsec^{-2}). The sensitivity of the SQM does not match either the standard responses of commonly used astronomical bands, or the human scotopic or photopic sensitivities (Cinzano 2005). For this reason, the 'luminance' measurements reported by the SQM should be considered to be instrument specific. In this paper, we use ratio techniques to make conclusions that are independent of the actual sky radiance.

With a quoted systematic uncertainty of 10 per cent, the SQM is not designed as a precision device. This uncertainty, however, is small compared to the night-to-night variations caused by cloud cover (which are a factor of 10 at our measurement location) and by distance from the city centre (a factor of 6 difference between our urban measurement location and another 32 km from the city centre) (Kyba et al. 2011a; Lolkema et al. 2011). The SQM is calibrated by the manufacturer before delivery,[2] and an inexpensive weatherproof housing is available from the manufacturer.

Although the two lightmeters have the same goal of measuring the brightness of the nighttime sky, they are not equivalent. The primary strength of the SQM is that by restricting measurements towards the zenith, it is far easier to find suitable measurement locations. Assuming, however, that a suitable site can be found, the self-calibration feature of the IYA lightmeter makes it a superior device for studying subtle changes in the night sky over many years. Given that the spectral response of the detectors does not match the human eye, any conversion of their measurements to lumens or lux is necessarily approximate. Regardless of this, the last several years have seen hundreds of these light pollution detectors installed by light pollution researchers, professional and amateur astronomers, and environmental groups.

2 MATERIALS AND METHODS

2.1 Light detectors and filters

We have constructed a prototype multispectral light pollution detector by pairing several SQM-LU light pollution meters with colour filters. We chose the SQM over the IYA lightmeter because it should be easy to replace the current IR filter with a colour filter in a future version of the SQM. Further, since the photosensitive element and the filter are both inexpensive, it should be possible to manufacture a scaled up version of the SQM that makes use of multiple photodetectors without a great increase in cost.

Four SQM-LUs were specially manufactured and calibrated for this experiment by Unihedron (each of which had their IR blocking filters removed) and a fifth standard SQM-LU for comparison. Each SQM was inserted into a weatherproof housing and attached to the outside of a metal frame, as shown in Fig. 2. The base of the frame was aligned using a water level to achieve an orientation as close to zenith as possible. An IYA lightmeter was also later installed, but the data from this instrument are not considered in this paper. The SQMs and IYA lightmeter were read out by a laptop installed in a weatherproof box attached to the same frame, and the entire apparatus was installed on the roof of our building at the Freie Universität (52.4579°N, 13.3111°E, 77-m elevation).

We obtained four scientific grade filters from Finger Lakes Instrumentation, with reported transmission in luminous (370–700 nm),

Figure 2. Prototype detector set-up. Five SQMs are securely fixed to a weatherproof box, which contains the acquisition computer. Each of the SQMs views the sky through a different filter: from left to right the standard SQM filter, a luminous filter, and red, green and blue filters. (The red filter appears blue in the photo because the red light has been transmitted and absorbed at the detector.) After this photo was taken, an IYA lightmeter was attached to the top left side of the weatherproof box.

[2] The manufacturer reports that units returned later for testing provide measurement within the quoted uncertainty, except in cases when water or moisture had entered the unit. Private communication with Anthony Tekatch.

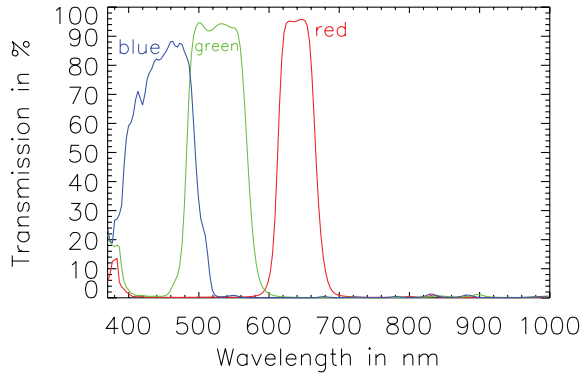

Figure 3. Transmission curves for the colour filters. The lamp used for these measurements did not emit sufficient ultraviolet light for accurate measurements to be made. The observed transmission below 400 nm for the red and green filters is believed to be an artefact.

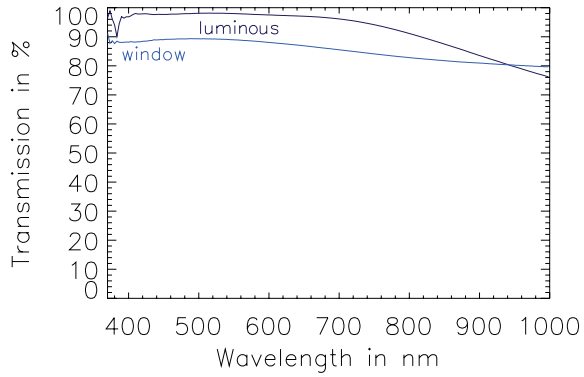

Figure 4. Transmission curves for the luminous filter (luminous) and for the weatherproof window of the SQM housing (window). The luminous filter was expected to have a strong cut-off at 700 nm, but instead passes a large amount of IR light.

red (590–690 nm), green (490–580 nm) and blue (370–510 nm) (LRGB) bands. The primary reason for using these filters, which do not correspond to standard filters used in astronomy, is that we used identical filters for both measurement of the polarization of the night sky in different spectral channels (Kyba et al. 2011b) and for aerial surveys of light pollution sources (Kuechly et al. 2012). To fit into our program of comparing ground-based to aerial measurements, it was important that the wavelength ranges be the same between the different experiments. For the purposes of demonstrating the feasibility of an inexpensive multichannel light pollution detector, the choice of filters is not important. However, if such a device is eventually developed for mass production, it would be advisable that the sensitivity matches standard astronomy bands to the greatest extent possible, while at the same time keeping the overall cost of the device low to ensure the possibility of widespread adoption.

We measured the transmission of the LRGB filters, and the results are shown in Figs 3 and 4. The measured transmission ranges for the colour filters were similar[3] to that reported by the distributor (www.flicamera.com/filters/index.html), although the maximum transmission we observed for the blue band was lower than reported. It should be noted that the red filter does not have strong transmission at the 589-nm line produced by low-pressure sodium lamps (Elvidge et al. 2010). The transmission of the luminous filter shown in Fig. 4 did not match the advertised curve at all, and allowed significant IR light to reach the sensor. The transmission of the window used for the weatherproof SQM housing varies little over the range of peak SQM response.

The LRGB filters were inserted between the SQM and the transparent window of the SQM housing, and were held in place by friction. The cap of the housing attaches firmly, and we observed no shifting of the filters over the course of the measurement. The windows were cleaned at the start of 2011 May as a noticeable amount of pollen had been deposited. The windows were not cleaned again until a controlled cleaning experiment was done at the start of 2011 October.

The SQM reports its luminance measurements in units of mag arcsec^{-2}, a logarithmic astronomical unit well known to light pollution researchers. The mag arcsec^{-2} scale is defined in such a way that an *increase* of 5 mag arcsec^{-2} corresponds to a *decrease* in sky luminance by a factor of 100. The unit can be approximately converted into cd m^{-2} using the formula $\mathrm{cd\,m^{-2}} = 9.0 \times 10^4 \times 10^{-0.4x}$, where x is the luminance in mag arcsec^{-2}, but it should be noted that this equation contains an implicit assumption about the observed wavelength distribution. Since we are not interested in absolute measurements, but are rather comparing the results of individual SQMs at different time periods, we simply report unitless 'amplification factors' (AF), using the formula $\mathrm{AF} = 10^{0.4\Delta x}$, where Δx is the difference in mag arcsec^{-2} between the two measurements.

2.2 Data acquisition

The experimental apparatus was entirely self-contained, with a power connection the only cable being connected. The weatherproof box containing the read-out computer acted as an imperfect Faraday cage, and a constant wireless connection could not be maintained as was planned. The data were therefore transferred periodically using a USB flash drive, and the time was maintained by the computer's internal clock. This clock was at first not properly calibrated, and drifted at a rate of −15 s per day. After calibrating the clock, we observed a drift rate of approximately −0.1 s per day. The timestamps for data taken before the clock was calibrated were linearly adjusted to remove the drift.

The SQMs were read out using a custom PERL script, based on an example provided by the manufacturer. The devices were sampled approximately once per second, and the data were written to separate ASCII log files for each SQM. Once installed, the IYA lightmeter was also read out once per second, using C code provided by Günther Wuchterl.

2.3 Alignment and cross-calibration

The SQMs were read out for two nights prior to installing the filters, in order to test both the alignment of the devices and to perform a rudimentary cross-calibration. The original agreement was excellent, as can be seen in Fig. 5. The upper plot compares data taken with the four filterless SQMs on the night of 2011 April 1, between midnight and 06:00 local time (UTC+2). The rapid variation was due to the passage of scattered clouds across the field of view of the SQMs, and the fact that almost all of the data are overlapping shows that the SQMs were viewing the same cloud patterns. The lower plot is a zoom-in of the period from 04:00 to 05:00 to show the fine differences between the SQMs. The four

[3] Our spectrometer has not been calibrated in several years, and measurements with line lamps indicated that there is an uncertainty of ∼3 nm in wavelength.

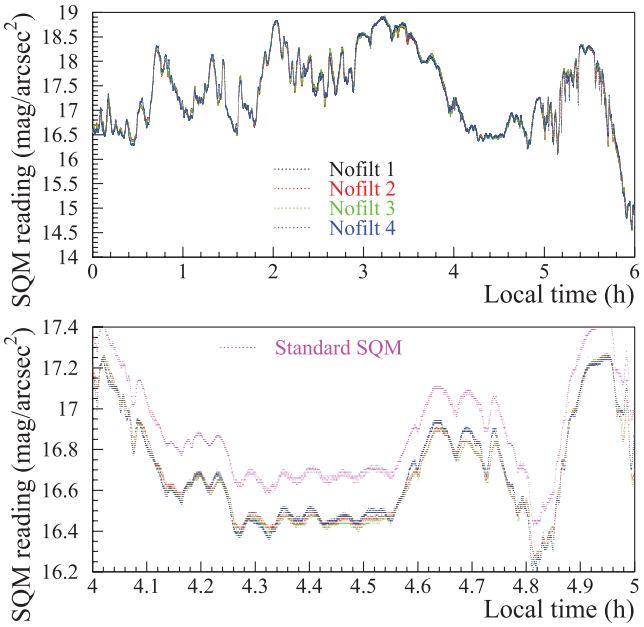

Figure 5. Comparison of the SQM uniformity and alignment at the start of the experiment. The upper plot shows the data observed on a partly cloudy night for the four SQMs with no filter installed. The lower plot shows a zoomed-in view of 1 h, and compares the four filterless SQMs to the SQM with the standard filter. Note that larger values of mag arcsec^{-2} indicate darker skies, as can be seen in the rapid onset of sunrise in the upper plot.

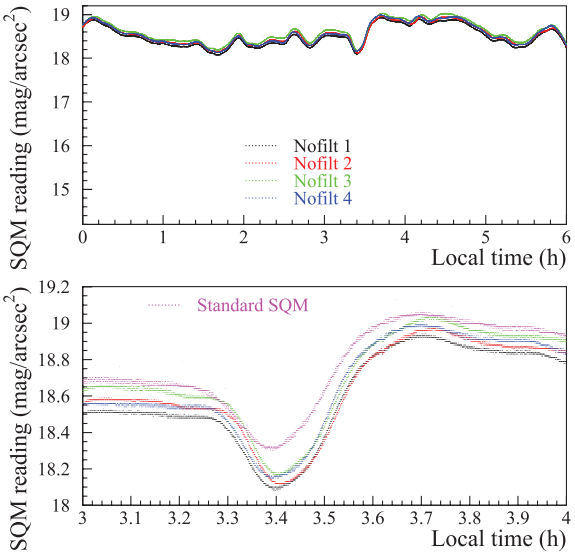

Figure 6. Comparison of the SQM uniformity and alignment at the end of the experiment. The scales are the same as in Fig. 5. The values recorded by the SQMs are no longer in excellent agreement, but the differences are still very small compared to the intrinsic variation of the urban night sky. Note that larger values of mag arcsec^{-2} indicate darker skies.

filterless SQMs agree with each other far better than the quoted systematic uncertainty (0.1 mag arcsec^{-2}). Note that the blue points appear both below and above the green points (e.g. at local times 4.3 and 4.4 h, respectively), indicating that the observed differences are likely due to some degree of misalignment rather than a unit-to-unit difference. The lower plot also shows the values observed for the SQM with the standard filter. This SQM showed the same variability with cloud formation, but reported larger values of mag arcsec^{-2}, as the IR filter reduces the amount of light incident upon the sensor (a decrease in mag arcsec^{-2} corresponds to an increase in measured sky luminance). The agreement seen here is better than that reported in a recent comparison of nine SQMs (den Outer et al. 2011). This could possibly be attributed to the fact that the SQMs used in this study were all from the same batch, and were installed very shortly after calibration by the manufacturer.

At the start of the fall season (2011 September 28), the filters were removed in order to check if the SQMs were still in good agreement. Before removing the filters, it was noted by eye that the alignment of the SQMs had shifted to a small extent compared to that shown in Fig. 2. Because the housing must be physically manipulated in order to remove the filter, it is likely we further changed the alignment, but at this stage we did not attempt to correct the alignment in any way. The results for the morning of 2011 September 29 are shown in Fig. 6. We calculated the average deviation of each of the unfiltered SQMs from the mean value for the period in the right-hand panel (similar to, but much less rigorous than, the intercalibration of den Outer et al. 2011). The difference in mean deviation between the two largest outlying SQMs was 0.1 mag arcsec^{-2}, and the sample standard deviation was $\sigma = 0.04$ mag arcsec^{-2}, which is still less than half the quoted unit-to-unit uncertainty of 0.1 mag arcsec^{-2}.

Visual inspection of the SQMs at the time the filters were removed showed that the windows of the SQM external housings were no longer transparent, due to the deposition of pollen or dust. We cleaned the SQMs on October 1 between 22:45 and 23:00 and then again during the day on October 4 (when we were better able to inspect the windows). Since we have an additional SQM-LE monitoring the night sky in almost the same location (Kyba et al. 2011a), we compared the differences between each of our filterless SQM-LUs to that SQM-LE before and after cleaning (i.e. a difference of differences). We found that cleaning increased the measured value of sky luminance by approximately 0.13 mag arcsec^{-2}, a transmission difference of ∼12 per cent.

After cleaning, we compared the deviation of the four filterless SQMs to their average value during the clear sky period from 00:00 to 05:00 local time on October 3. The mean deviation between the two most outlying SQMs was 0.074 mag arcsec^{-2}, and the sample standard deviation was $\sigma = 0.03$ mag arcsec^{-2}. We will continue to monitor these SQMs over the next several years to test whether their calibration remains accurate.

2.4 Cloud coverage analysis

As shown in Fig. 1, the effect that clouds have on ground-level illumination in urban areas is the reverse of what occurs in natural areas. In a previous paper we showed that at our measurement location at the Freie Universität in the summer of 2010, fully overcast skies were 10.1 times more luminous than clear skies (Kyba et al. 2011a). That analysis was done using an SQM-E with the standard filter, and a much wider field of view. We have repeated the analysis described in Kyba et al. (2011a) for each of the five different filters.

To briefly summarize the method, the SQM data were first binned into 1-min averages. To avoid the unnecessary complication of moonlight, we analysed only data for which the Moon was at least 2° below the horizon. The Moon's position[4] was calculated using the PERL program 'Astro::Coord::ECI::Moon' (v0.043, freely available from the Comprehensive Perl Archive Network), written by Thomas

[4] When the Moon is above the horizon, the code takes refraction into account. Below the horizon the code returns the Moon's true elevation.

Table 1. Frequency of cloud coverage conditions over the course of data taking.

Oktas	0	1	2	3	4	5	6	7	8
Total nights	31	28	11	11	11	11	14	35	26
Moonless nights	20.2	15	6	4	3.5	5	4.1	17.8	10

Note. For each value of cloud coverage (0 is clear, 8 is overcast), the number of nights in the observation period is shown, along with the effective number of nights that the Moon was at least 2° below the horizon between 00:45 and 01:15 (UTC+2). Fractional values occur due to nights in which the Moon rose or set during this time period.

R. Wyant and based on the algorithms of Meeus (1991). Since we have previously observed that the sky over Berlin becomes darker as the night progresses, we restrict our cloud coverage analysis to time periods between 00:45 and 01:15 local time (UTC+2, Central European Summer Time). Cloud coverage figures were determined by a human observer at a manned weather station located adjacent to our measurement location (Berlin-Dahlem, World Meteorological Index 10381), and were retrieved from the OGIMET web site, http://www.ogimet.com.

The experimental time period began on the night of April 1 and 2, and continued until the night of September 26 and 27. The data from one night are not included (April 21 and 22) because the meteorological observation was missing, giving a total of 178 observing nights. After rejecting data that included moonlight and restricting the analysis to within 15 min of 01:00 local time, 2565 minute-by-minute observations remained. The frequency of each level of cloud cover is shown with the effective number of moonless nights in Table 1. Clear (0–1 okta), partly cloudy (2–6 okta) and overcast skies (7–8 okta) occurred with almost equal frequency.

The degree of light pollution at zenith at the experimental site corresponds to approximately 10 times the natural sky brightness. We consider only moonless nights because at this level of light pollution the presence of scattered moonlight would strongly affect the results. However, variations in other factors affecting the level of natural light (e.g. position of the Milky Way, variations in the intensity of the 557.7-nm airglow line) are small in comparison to other environmental variations, such as aerosol concentrations, changes in the total light emitted by the city and changes in the ground albedo and leaf shading. If a similar experiment were to be performed in a dark sky area, the natural changes in sky radiance at zenith would have a much stronger effect and would need to be taken into account.

2.5 Nightly colour change analysis

For reasons as yet unknown to us, the zenith sky luminance in Berlin greatly decreases as the night progresses. We have previously surmised that this was due to sport, residential, automobile and advertising lighting being turned off as residents went to bed (Kyba et al. 2011a). It has also been suggested that gradual changes could also be due to changes in the atmospheric properties, notably the height of the planetary boundary layer (McKenna 2008).

Since nightly changes in zenith sky luminance are not well understood, we decided to test whether the different spectral channels see the same changes in luminance. To do this, we identified moonless (lunar elevation $< -2^\circ$), cloud-free (0 okta) data for which the Sun was at least 16° below the horizon, using the same date range as in the cloud analysis (2011 April 1 to September 26). The requirement for the Sun to be at least 16° was determined using a similar analysis to that presented in Lolkema et al. (2011). For each filter, we found the median observed luminance (in mag arcsec^{-2}) within 5 min of 'true' local midnight (01:00 local time), and used this to create profile histograms of the luminance relative to this time. Note that due to these selection criteria the number of observations for any given time period (e.g. 01:55–02:00 versus 02:00–02:05) is not constant, nor are the dates from which the data are drawn.

3 RESULTS AND DISCUSSION

The cloud AF for each wavelength range and level of cloudiness is shown graphically in Fig. 7. Thin horizontal lines show the median observed value, and thick (thin) vertical lines show the spread of 68.3 per cent (95.5 per cent) of all the data that passed the selection cuts. The median values are also shown in Table 2. The figure and table show that the increased luminance of the sky due to clouds is the strongest for long wavelengths. This is due to the fact that short wavelengths are more easily Rayleigh scattered on clear nights, and the normalization is relative to clear skies. In other words, the radiation that escapes to space on clear nights is biased towards long wavelengths, and the effect of clouds is to redirect this predominantly red light back towards the city.

Cloud cover and snow cover are the most important factors affecting the radiance of the urban nocturnal sky on moonless nights.

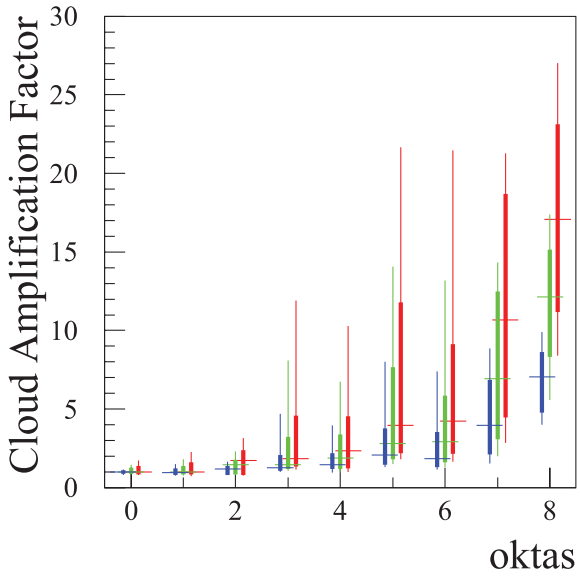

Figure 7. Increase in sky brightness due to cloud coverage. The plot shows the ratio of the observed sky luminance to the median value observed for clear Berlin skies (at 52.4579°N, 13.3111°E from 2011 April 1 to September 26) for the blue, green and red filters (from left to right), respectively. Horizontal lines show the median value and vertical bars show the spread of the data.

Table 2. Amplification factor of clouds by filter colour.

Oktas	0	1	2	3	4	5	6	7	8
HOYA CM-500	1	1.0	1.5	1.5	2.0	3.2	3.0	7.4	11.6
Luminous	1	1.0	1.5	1.6	1.9	3.6	3.2	8.8	14.6
Red	1	1.0	1.7	1.9	2.4	4.0	4.3	10.7	17.6
Green	1	1.0	1.5	1.5	1.9	2.8	2.9	6.9	12.1
Blue	1	1.0	1.2	1.3	1.5	2.1	1.9	2.9	7.1

Note. For each value of cloud coverage (0 is clear, 8 is overcast), the median factor by which clouds increase the luminance of the sky (relative to clear skies) is shown.

Nevertheless, there exists a significant variation in the measured radiance on clear summer moonless nights. These variations could be due to many factors, including the presence of aerosols, the humidity, public behaviour (e.g. events, or weekend versus weekday), changes in ground albedo and foliage cover and, as we have shown in Section 2.3, the length of time since the SQM window was cleaned. Because of the large number of variables involved and the relatively small number of clear moonless summer nights, considerably more observation time will be needed before the relationships between sky radiance and these variables will be able to be tested.

One of our primary goals in producing this data set is to obtain measurements for testing a future light pollution model of Berlin in different wavelength channels and atmospheric conditions. Ratio measurements suffice for this purpose. However, if our measurement equipment was radiometrically calibrated it would have several additional applications. One obvious example is to estimate the dose of 'circadian light' (Rea et al. 2010) that an organism living outside would be exposed to over the long term. Since the eye sensitivity of other animals does not match the human eye, information in several wavelength channels in combination with a light pollution model could allow one to generate geographic maps of skyglow 'illuminance' for individual organisms (e.g. to predict the behaviour of fish and zooplankton; Boscarino et al. 2009). Finally, it has been reported that anthropogenic night light can photolyse tropospheric NO_3 (Stark et al. 2011). The increase in irradiance brought about by cloud reflection of light pollution can be expected to increase the rate of NO_3 photolysis, but since the interaction probability is wavelength dependent (Johnston et al. 1996) one would need multispectral measurements through the nighttime period to calculate photolysis rates accurately.

With this in mind, we now consider our measurement of the changes in sky luminance over the course of the night, as described in Section 2.5. The top plot of Fig. 8 shows the luminance relative to the middle of the night ($t = 0$, 01:00 local time) over the course of 6 h. The vertical error bars show the standard deviation of the mean (the spread in the data is much larger). The bottom plot shows the number of observations that satisfied the selection criteria (cloud-free and moonless) 1-min averages. Because the Sun does not achieve low elevations during the summer, more data are available towards the middle of the night. Even on clear nights urban sky luminance is quite variable, so it is unsurprising that the trend breaks down when only a small number of nights from spring or fall are included.

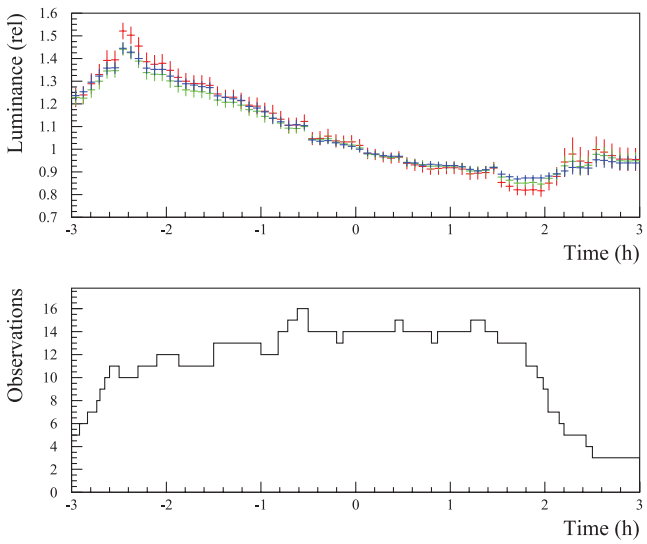

Figure 8. Changes in sky luminance over the course of the night. The top plot shows the ratio of the observed sky relative to the luminance observed in the middle of the night ($t = 0$, 01:00 local time) for the red, green and blue filtered data, for portions of selected clear nights as described in Section 2.5. Vertical error bars show the standard deviation of the mean. Note that the zero is suppressed to make the trend more clear. The bottom plot shows the number of observations (nights) satisfying the selection criteria.

We fit the data for the standard SQM-LU (it is not shown in Fig. 8, but the trend is similar) using a piecewise linear fit. The fit result for the data from 23:00 to 00:30 local time ($-2 < t < -0.5$) was a luminance decrease of 16.3 ± 1.4 per cent per hour, and from 00:30 to 03:00 ($-0.5 < t < 2$) was a slower decrease of 7.7 ± 0.5 per cent per hour. Both percentages are relative to the value observed in the middle of the night.

It appears that the rate of decrease in red light is greater than in blue. While this is consistent with the hypothesis that the decrease in skyglow over the course of an evening is due to reductions in red-rich traffic and household incandescent lighting, at this point in time we prefer not to draw any conclusions, as a spurious difference could potentially be generated by differences in the time of year in which the data were acquired. This decrease would be best studied using a more sensitive spectrometer on individual perfectly clear nights, as it would be easier to identify trends related to the different individual light sources (e.g. low-pressure sodium lights are normally not used for residential lighting).

4 CONCLUSION

In this paper, we have demonstrated the widespread need for an inexpensive multispectral light pollution meter. The likely worldwide transition to increased LED street lighting may have an effect on research topics as diverse as biological chronodisruption and air pollution, and long-term monitoring of skyglow should start before the transition is well underway. We have shown that by combining filters with existing inexpensive light meters, multispectral measurements are possible. Although we used precision filters, for future versions of such a device inexpensive filters would likely suffice, assuming that their transmission is known adequately well.

We used our prototype multispectral luminance meter to show that in urban areas clouds have a much bigger impact on the amount of red light (17×) redirected towards the surface than blue (7×). We monitored the decrease in sky luminance over Berlin as the night progressed, and found that the rate of decrease appears to be greater for red light than blue, although it is possible that this result is due to a seasonal effect.

We urge manufacturers to consider bringing a device based on our prototype to market. It would be particularly useful if manufacturers of weather stations (which often include irradiance meters that are sensitive only during daylight) would consider offering a multispectral night light sensor as a part of a standard package.

ACKNOWLEDGMENTS

We thank Unihedron for producing and calibrating the non-standard filterless SQM-LUs. We also thank Sabrina Schnitt for her measurement of the filter transmissions, and Tom Wyant for developing the Astro::Coord::ECI code. This work was supported by the project *Verlust der Nacht* (funded by the Federal Ministry of Education and Research, Germany, BMBF-033L038A) and by focal area MILIEU (FU Berlin).

REFERENCES

Aubé M., 2007, in Marín C., Jafari J., eds, Proc. Starlight 2007 Conf. Light Pollution Modeling and Detection in a Heterogeneous Environment. La Palma, Spain

Berry R. L., 1976, J. R. Astron. Soc. Can., 70, 97

Bertiau F. C., de Graeve E., Treanor P. J., 1973, Vatican Obser. Publ., 1, 157

Boscarino B. T., Rudstam L. G., Eillenberger J. L., O'Gorman R., 2009, Aquat. Biol., 5, 263

Brainard G. C., Hanifin J. P., Greeson J. M., Byrne B., Glickman G., Gerner E., Rollag M. D., 2001, J. Neurosci., 21, 6405

Cinzano P., 2005, Technical Report 9, Night Sky Photometry with Sky Quality Meter. ISTIL

Cinzano P., Falchi F., Elvidge C. D., 2001, MNRAS, 328, 689

den Outer P., Lolkema D., Haaima M., van der Hoff R., Spoelstra H., Schmidt W., 2011, Sensors, 11, 9603

Duriscoe D. M., Luginbuhl C. B., Moore C. A., 2007, PASP, 119, 192

Elvidge C. D., Keith D. M., Tuttle B. T., Baugh K. E., 2010, Sensors, 10, 3961

Espen H., 2011, The Atlantic, July/August

Falchi F., 2010, MNRAS, 412, 33

Falchi F., Cinzano P., Elvidge C., Keith D., Haim A., 2011, J. Environ. Manage., 92, 2714

Gallaway T., 2010, J. Econ. Issues, 44, 71

Gallaway T., Olsen R. N., Mitchell D. M., 2010, Ecol. Econ., 69, 658

Gooley J. et al., 2011, J. Clin. Endocrinol. Metab., 96, E463

Haim A., Heth G., Pratt H., Nevo E., 1983, J. Exp. Biol., 107, 59

Herring H., Roy R., 2007, Technovation, 27, 194

Hölker F. et al., 2010, Ecol. Soc., 15(4), 13

International Dark-Sky Association, 2010, Technical Report, Visibility, Environmental, and Astronomical Issues Associated with Blue-Rich White Outdoor Lighting. International Dark-Sky Association, Tucson, AZ

Johnston H. S., Davis H. F., Lee Y. T., 1996, J. Phys. Chem., 100, 4713

Kantermann T., Roenneberg T., 2009, Chronobiol. Int., 26, 1069

Kloog I., Haim A., Stevens R. G., Barchana M., Portnov B. A., 2008, Chronobiol. Int., 25, 65

Kloog I., Haim A., Stevens R. G., Portnov B. A., 2009, Chronobiol. Int., 26, 108

Kocifaj M., 2011, MNRAS, 415, 3609

Kolláth Z., 2010, J. Phys. Conf. Ser., 218, 012001

Kuechly H., Kyba C. C. M., Ruhtz T., Lindemann C., Wolter C., Fischer J., Hölker F., 2012, Remote Sensing Environment, submitted

Kyba C. C. M., Ruhtz T., Fischer J., Hölker F., 2011a, PLoS ONE, 6, e17307

Kyba C. C. M., Ruhtz T., Fischer J., Hölker F., 2011b, J. Geophys. Res., 116, D24106

Lewy A. J., Wehr T. A., Goodwin F. K., Newsome D. A., Markey S. P., 1980, Sci, 210, 1267

Lolkema D., Haaima M., den Outer P., Spoelstra H., 2011, Technical Report RIVM 680151002, Effects of Meteorological and Atmospheric Parameters on Night Sky Brightness. Netherlands National Institute for Public Health and the Environment, Bilthoven, the Netherlands

Luginbuhl C. B., Lockwood G. W., Davis D. R., Pick K., Selders J., 2009, PASP, 121, 185

McKenna D., 2008, Technical Report, Current Status of the Vatican Observatory/IDA Night Sky Brightness Monitor (NSBM) As of 2008 October. International Dark-Sky Association, Tucson, AZ

Meeus J. H., 1991, Astronomical Algorithms. Willmann-Bell, Inc., Richmond, VA

Meng Y., He Z., Yin J., Zhang Y., Zhang T., 2011, Med. Biol. Eng. Comput., 49, 1083

Moore M. V., Pierce S. M., Walsh H. M., Kvalvik S. K., Lim J. D., 2000, Verh. Int. Verein. Limnol., 27, 779

Narisada K., Schreuder D., eds, 2004, Light Pollution Handbook, Vol. 322 of Astrophysics and Space Science Library. Springer, Berlin

Navara K. J., Nelson R. J., 2007, J. Pineal Res., 43, 215

Perkin E., Hölker F., Richardson J., Sadler J., Wolter C., Tockner K., 2011, Ecosphere, 2, 122

Rea M., Figueiro M., Bierman A., Bullough J., 2010, J. Circadian Rhythms, 8

Reddy A. B., O'Neill J. S., 2010, Trends Cell Biol., 20, 36

Reiter R., Tan D., Sanchez-Barcelo E., Mediavilla M., Gitto E., Korkmaz A., 2011, J. Exp. Integr. Med., 1, 13

Rich C., Longcore T., eds, 2006, Ecological Consequences of Artificial Night Lighting. Island Press, Washington, DC

Riegel K., 1973, Sci, 179, 1285

Salmon M., Tolbert M. G., Painter D. P., Goff M., Reiners R., 1995, J. Herpetol., 29, 568

Stark H. et al., 2011, Nat. Geosci., 4, 730731

Sumriddetchkajorn S., Somboonkaew A., 2010, Proc. SPIE, 7853, 78530L

Walker M., 1970, PASP, 82, 672

Walker C. E. et al., 2008, in Gibbs M. G., Barnes J., Manning J. G., Partridge B., eds, ASP Conf. Ser. Vol. 400, Preparing for the 2009 International Year of Astronomy: A Hands-On Symposium. Astron. Soc. Pac., San Francisco, p. 116

Wyse C., Selman C., Page M., Coogan A., Hazlerigg D., 2011, Med. Hypotheses, 77, 1139

Zotti G., 2007, in Mohar A., ed., DARKSKY2007 – 7th European Symp. for the Protection of the Night Sky Measuring Light Pollution with a Calibrated High Dynamic Range All-Sky Image Acquisition System

This paper has been typeset from a TEX/LATEX file prepared by the author.